33rd Annual International Conference of the IEEE EMBS
Boston, Massachusetts USA, August 30 - September 3, 2011

Non-invasive Prediction of Catheter Ablation Outcome in Persistent Atrial Fibrillation by Exploiting the Spatial Diversity of Surface ECG

Marianna Meo*, *Student Member, IEEE*, Vicente Zarzoso, *Senior Member, IEEE*,
Olivier Meste, *Member, IEEE*, Decebal G. Latcu, and Nadir Saoudi

***Abstract*— Atrial fibrillation (AF) is the most common cardiac arrhythmia encountered in clinical practice. Radiofrequency catheter ablation (CA) is becoming one of the most widely employed therapies. Yet selection of patients who will benefit from this treatment remains a challenging task. Previous works have examined several electrocardiogram (ECG) parameters as potential predictors of CA success, such as fibrillatory wave (f-wave) amplitude. However, they require a manual computation and consider only a subset of electrodes, so inter-lead spatial variability of the 12-lead ECG is not fully exploited. The present study puts forward an automatic procedure for f-wave amplitude computation to non-invasively predict CA outcome. An extension of this quantitative measure to the whole set of leads is also proposed, based on Principal Component Analysis (PCA). We show that exploiting the spatial diversity present in the surface ECG not only improves the robustness to electrode selection but also increases the predictive power of the amplitude parameter.**

I. Introduction

Atrial fibrillation (AF) is often regarded as the "last great frontier of cardiac electrophysiology". Neither its natural history nor its response to therapy are sufficiently predictable by clinical and echocardiographic parameters [1]. Nonpharmacological approaches based on radiofrequency catheter ablation (CA) are becoming increasingly popular and effective. During the procedure, radiofrequency energy is delivered through a catheter tip around the connections of the pulmonary veins (PVs) to the left atrium, known to be an important source of spontaneous electrical activity initiating AF [2], [3], so that sinus rhythm can be restored [4]. More recently, ablation based on the so-called Complex Fractionated Atrial Electrograms (CFAE) has also shown its efficacy in terminating AF [5], but clinical results reported by different centers performing the treatment are rather disparate [6]. These discrepancies have pointed out the need for strategies to select patients most likely to benefit from the therapy.

Previous studies have examined several parameters to predict CA outcome and select candidate patients for the treatment from the analysis of the fibrillatory waves (f-waves) observed in the surface ECG. In particular, the role of f-wave amplitude as an effective predictor of procedural AF termination has been assessed in [7]. Nonetheless, these methods rely on manual measurement of parameters in the recorded ECG, which increases subjectivity and error probability. Secondly, only individual leads (such as V_1 and II) are selected for this analysis, so inter-lead variability is not taken into account.

To overcome these drawbacks, the present study aims at a fully automatic acquisition of the f-wave amplitude on the surface ECG. We first propose an algorithm to quantify the f-wave peak-to-peak amplitude on a single lead. This algorithm is based on cubic spline interpolation of the local extrema of the atrial signal observed in surface recordings. Using Principal Component Analysis (PCA), the algorithm is then extended to multilead recordings, so that the spatial diversity of the ECG can also be exploited. CA prediction results on a persistent AF ECG database prove consistent with those obtained by manual measures in [7] and show the advantages of considering more than one lead in the amplitude analysis.

II. Methods

A. ECG Data and Acquisition System

A dataset of 18 male patients suffering from persistent AF was employed in this study. They all underwent CA, performed with the aid of Prucka Cardiolab and Biosense CARTO electrophysiology measurement systems at the Cardiology Department of Princess Grace Hospital in Monaco. Surface ECG signals were acquired in several crucial moments of the treatment, namely, at the beginning, after PV isolation and at the end of the surgery, through a standard 12-lead system at a sampling rate of 1 kHz. Fourteen patients experienced AF termination, either spontaneously obtained after the operation or externally induced by electrical cardioversion or drug treatment. The study endpoint was short term procedural success, defined as AF termination by CA either directly to sinus rhythm or to intermediate atrial tachycardia(s) within a 3-month blanking period.

B. ECG Preprocessing and Atrial Activity Segmentation

Firstly, input signals were filtered by using a forth-order zero-phase Chebyshev bandpass filter with a -3 dB attenuation at 0.5 Hz and 30 Hz cut-off frequencies. This passband retains the most significant AF content, wose dominant frequency ranges between 3 and 12 Hz, while suppressing baseline wandering and high frequency noise

Manuscript received April 15, 2011. This work is partly supported by the French National Research Agency under contract ANR-2010-JCJC-0303-01 "PERSIST". Marianna Meo is funded by a doctoral grant from the French Ministry of Higher Education and Research.

*Marianna Meo, Vicente Zarzoso and Olivier Meste are with the Laboratoire d'informatique, signaux et systèmes de Sophia Antipolis (I3S), Université Nice Sophia Antipolis, CNRS, France (e-mail:{meo, zarzoso, meste}@i3s.unice.fr).

Decebal G. Latcu and Nadir Saoudi are with the Service de cardiologie, Centre Hospitalier Princesse Grace, Monaco (e-mail: {dglatcu, nsaoudi}@chpg.mc).

978-1-4244-4122-8/11/$26.00 ©2011 IEEE

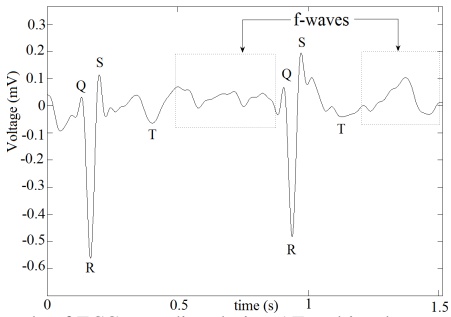

Fig. 1: Example of ECG recording during AF and its characteristic waves. Dotted boxes highlight TQ intervals which are concatenated to form the AA signal $\mathbf{Y}_{\mathrm{AA}}$ in Equation (1).

like myoelectric artifacts and 50 Hz power line interference. Then, R wave time instants were located on lead V_1 by means of Pan-Tompkins' algorithm [8]. Afterwards, Q wave onset and T wave offset were detected with an improved version of Woody's method [9], so as to properly segment the TQ intervals. These segments were subsequently mean-corrected and concatenated to form the signal representing atrial activity (AA), as in Fig. 1. This preprocessing stage was justified by our interest in studying f-wave amplitude properties, regardless of their temporal location or time coherence. In this manner, an $(L \times N)$ data matrix $\mathbf{Y}_{\mathrm{AA}}$ can be defined as:

$$\mathbf{Y}_{\mathrm{AA}} = [\mathbf{y}_{\mathrm{AA}}(1) \cdots \mathbf{y}_{\mathrm{AA}}(N)] \in \mathbb{R}^{L \times N} \tag{1}$$

where vector $\mathbf{y}_{\mathrm{AA}}(t) = [y_1(t), \ldots, y_L(t)]^T$ represents the multilead AA signal measured at time instant t, L denotes the number of leads considered (e.g., $L = 12$ for the standard ECG), and N the number of samples of the AA signal $y_\ell(t)$ for each lead $\ell = 1, 2, \ldots, L$.

C. Automatic f-wave Amplitude Computation

Previous works have demonstrated that the higher is f-wave peak-to-peak amplitude on the surface ECG, the more likely is the procedure to be successful [7]. However, the computation of this parameter is not always a trivial task, as waveform patterns can be quite irregular and complex. To surmount these difficulties, we propose an automatic algorithm consisting of the following steps. Given a signal $y(t)$, e.g., one of the atrial ECG leads $y_\ell(t)$, $\ell = 1, 2, \ldots, L$, an upper envelope $e_{\mathrm{MAX}}(t)$ is first estimated by piecewise cubic spline interpolation between the detected local maxima points. The same operation is repeated for the minima to generate a lower envelope $e_{\mathrm{MIN}}(t)$. This technique was designed to detect f-wave local extrema, without involving spurious peaks or signal artefacts into the computation. The two curves allow us to depict their main peaks and troughs, so their difference outlines the general trend of the most significant oscillations. Further extrema are added by mirror symmetry with respect to the extrema close to the end points of the whole recording, so as to prevent the propagation of numerical artifacts due to finite length observations. Then, another curve $e_{\mathrm{DIFF}}(t)$ is computed as the difference $e_{\mathrm{DIFF}}(t) = e_{\mathrm{MAX}}(t) - e_{\mathrm{MIN}}(t)$, and its values are finally averaged over the AA signal length N, yielding $D(y)$ as final output parameter $D(y) = \frac{1}{N}\sum_{t=1}^{N} e_{\mathrm{DIFF}}(t)$. The operator $D(\cdot)$ that we have just defined fulfills the property:

$$D(ky + \alpha) = |k| D(y), \quad \forall k, \alpha \in \mathbb{R}. \tag{2}$$

One advantage of our method is that index D condenses the information about f-wave variability over the whole recording and its peak-to-peak amplitude pattern in a single objective parameter.

D. Extension to Multilead Recordings

Another drawback of previous works is that f-wave amplitude is computed on single leads (e.g., V_1 or II), so its estimation is subject to the intrinsic variability of the surface ECG across different leads. To increase robustness to such variability, we propose to extend the method presented in the previous section to compute an average amplitude over more than one lead. The basic idea behind this extension is to exploit the ability of Principal Component Analysis (PCA) to decompose a given multivariate observation into sources or components with maximum variance [10]. Since variance is closely related with amplitude, the dominant principal components are expected to provide a sensible measure of the average amplitude of the atrial signal over the leads considered.

Mathematically, PCA obtains the following bilinear decomposition for the multilead recording stored in matrix $\mathbf{Y}_{\mathrm{AA}}$:

$$\mathbf{y}_{\mathrm{AA}}(t) = \mathbf{M}\mathbf{x}(t) = \sum_{k=1}^{L} \mathbf{m}_k x_k(t). \tag{3}$$

In this expression, $x_k(t)$ is the kth principal component (PC) of the multilead recording. The principal direction stored in the column $\mathbf{m}_k$ of $\mathbf{M}$ represents the relative contribution of $x_k(t)$ to the leads in $\mathbf{y}_{\mathrm{AA}}(t)$, $k = 1, 2, \ldots, L$, and so it can be considered as its propagation direction or spatial topography [11], [12]. In the sequel, we make the hypothesis that the dominant PC condenses the global amplitude of the AA present in the leads considered, as it is characterized by the maximum variance. Truncation of Equation (3) at the first PC results in the rank-1 approximation $\hat{\mathbf{y}}_{\mathrm{AA}}(t) = \mathbf{m}_1 x_1(t)$, which exclusively accounts for the contribution of the first source to the selected leads. Its waveform pattern is then examined and the average of peak-to-peak amplitude envelope values are computed on each lead as described in the previous section. This results in the L-component vector D_L defined as:

$$D_L = [d_1, d_2, \ldots, d_L]^{\mathrm{T}} \qquad d_\ell = D(m_{\ell 1} x_1) \tag{4}$$

where $m_{\ell 1} = [\mathbf{m}_1]_\ell$ is the ℓth element of vector $\mathbf{m}_1$. D_L entries are finally averaged to provide index $\overline{D}_L$ given by:

$$\overline{D}_L = \frac{\sum_{\ell=1}^{L} d_\ell}{L} = \frac{\sum_{\ell=1}^{L} |m_{\ell 1}| D(x_1)}{L} = \frac{\|\mathbf{m}_1\|_1}{L} D(x_1). \tag{5}$$

where $\|\mathbf{m}_1\|_1$ is the L1-norm of $\mathbf{m}_1$. Hence, the spatial distribution of f-wave amplitudes over the observed leads is condensed into a single index [Equation (5)] made up of the amplitude of the dominant principal component and the L1-norm of its spatial topography.

TABLE I: Interpatient statistical analysis

	AF termination	Non AF termination	p-value
$D(\mathrm{V_1})_{\mathrm{START}}$	0.072 ± 0.021	0.053 ± 0.021	0.128
$D(\mathrm{V_1})_{\mathrm{PV}}$	0.068 ± 0.020	0.046 ± 0.015	0.073
$D(\mathrm{V_1})_{\mathrm{AFTER}}$	0.068 ± 0.019	0.049 ± 0.017	0.090
$RMS(\mathrm{V_1})_{\mathrm{BEFORE}}$	0.037 ± 0.008	0.041 ± 0.023	0.766
$RMS(\mathrm{V_1})_{\mathrm{PV}}$	0.037 ± 0.010	0.034 ± 0.013	0.617
$RMS(\mathrm{V_1})_{\mathrm{AFTER}}$	0.042 ± 0.018	0.030 ± 0.006	0.063
$(\overline{D}_{12})_{\mathrm{START}}$	0.035 ± 0.016	0.018 ± 0.010	0.034
$(\overline{D}_{12})_{\mathrm{PV}}$	0.035 ± 0.015	0.025 ± 0.005	0.087
$(\overline{D}_{12})_{\mathrm{AFTER}}$	0.035 ± 0.017	0.024 ± 0.006	0.087

E. Statistical Analysis

Values of the aforementioned parameters have been expressed as mean $\pm$ standard deviation for each of the clinical cases "AF termination" and "non AF termination". CA outcome classification performance was evaluated by determining ROC curve parameters, such as the Area Under Curve (AUC) and the p value under a test confidence level α equal to 0.05. First, data Gaussianity was verified through Lilliefors' test. Differences between successful and failing CA procedures were statistically assessed by an unpaired Student's t-test for parametric data and a two-sample Kolmogorov-Smirnov test for non-parametric data. The statistical analysis was performed under the assumption $\alpha = 0.05$. Subscripts START, PV and END correspond to different CA phases, namely, before starting the procedure, after PV ablation and after completing the procedure.

III. Results

For the sake of comparison with previous works, $D(y)$ was evaluated on lead $\mathrm{V_1}$. Parameters were computed for each CA step and for every patient. Results are reported in Table I, together with p values of each unpaired test. For comparison, we also consider a standard method for amplitude computation, namely, the root mean square (RMS) value. The AUC values are shown in Table II. The multilead perspective of Section II-D was also tested and its performance compared with the single-lead approach. To this end, our algorithm was executed several times by exploiting different ECG lead subsets of increasing size L, ranging from 1 up to 12. At each subset dimension L, every possible L-lead subsets present in the ECG was considered, a total of $12!/((12-L)!L!)$ possible combinations. Parameter $\overline{D}_L$ in Equation (5) was computed for each possible L-lead subset for each patient. Prediction performance was then assessed for each lead combination from the corresponding values of $\overline{D}_L$. In this manner, the minimum, maximum and mean AUC values over all L-lead subsets were obtained as a function of the subset dimension L. The same analysis steps were repeated for each CA phase. AUC results are plotted in Fig. 2, while the lead combinations providing the best prediction performance for each subset dimension are shown in Table III. Tables I–II also compare the single-lead and 12-lead ECG analysis ($\overline{D}_{12}$).

IV. Discussion

F-wave amplitude is regarded as a CA outcome predictor. Recent works manually compute this parameter on a single ECG lead. The present study aimed at an innovative approach to predict CA short-term outcome by computing this parameter automatically and exploiting the spatial variability offered by the surface 12-lead ECG through source separation by PCA. The existence of a relation between the atrial wave amplitude on the surface ECG and AF clinical outcome has been confirmed by our work. Higher D values can be associated with AF termination by CA, regardless of the procedural moment considered, as shown in Table I. Even though statistical significance is not demonstrated for $D(\mathrm{V_1})$, experimental results are consistent with state of the art studies, which reported a mean amplitude value equal to 0.08 ± 0.03 mV on lead $\mathrm{V_1}$ in patients experiencing procedural success, $0.05 \pm 0.03mV$ otherwise (AUC $= 0.77$, $p < 1 \cdot 10^{-3}$) [7]. Nonetheless, unlike previous works, our analysis is completely automatic, and so able to output more objective results. Table II shows that parameter D can effectively predict CA clinical outcome, with results similar to those reported in [7]. In order to demonstrate the superiority of D over other parameters proportional to signal amplitude, in Table I a comparison with RMS values is drawn as well. Not only p values related to the unpaired tests are considerably higher than those computed for D (except for the post-operative phase), but RMS numerical results strongly differ from those presented by previous works [7]. In consequence, the hypothesis that higher amplitude values predict procedural AF termination cannot be evinced by such values, so it emerges that RMS is not capable of capturing the predicting properties of f-wave amplitude.

As far as $\overline{D}_{12}$ is concerned, classification of successful and failing cases before CA application is statistically significant, as shown in Table I. Figure 2 shows the classification performance of $\overline{D}_L$, which improves as the number of leads increases. The best results were obtained before performing CA. Our classifier improves its performance when using more than one lead, as AUC is generally maximum if L ranges between 2 and 8. These results demonstrate that a deeper insight into the pathology can be gained by adopting a multilead approach. Identical remarks can be made after CA execution. On the contrary, as far PV isolation step is

TABLE II: CA outcome prediction performance

	AUC	p value
$D(\mathrm{V_1})_{\mathrm{START}}$	0.75	$2 \cdot 10^{-2}$
$D(\mathrm{V_1})_{\mathrm{PV}}$	0.80	$3 \cdot 10^{-3}$
$D(\mathrm{V_1})_{\mathrm{AFTER}}$	0.79	$8 \cdot 10^{-3}$
$(\overline{D}_{12})_{\mathrm{START}}$	0.84	$4 \cdot 10^{-4}$
$(\overline{D}_{12})_{\mathrm{PV}}$	0.73	$4 \cdot 10^{-2}$
$(\overline{D}_{12})_{\mathrm{AFTER}}$	0.80	$3 \cdot 10^{-3}$

TABLE III: ECG lead subsets maximizing AUC

Number of Leads	Before CA	PV isolation	After CA
1	$\mathrm{V_3}$	$\mathrm{V_1}$	$\mathrm{V_2}$
2	II,$\mathrm{V_3}$	$\mathrm{V_1}$,$\mathrm{V_3}$	III,$\mathrm{V_2}$
3	II,$\mathrm{aV_L}$,$\mathrm{V_3}$	$\mathrm{aV_L}$,$\mathrm{V_1}$,$\mathrm{V_3}$	$\mathrm{aV_L}$,$\mathrm{aV_F}$,$\mathrm{V_2}$
4	II,$\mathrm{aV_L}$,$\mathrm{V_3}$,$\mathrm{V_4}$	III,$\mathrm{V_1}$,$\mathrm{V_3}$,$\mathrm{V_5}$	III,$\mathrm{aV_L}$,$\mathrm{V_3}$,$\mathrm{V_6}$
5	II,$\mathrm{aV_L}$,$\mathrm{V_3}$, $\mathrm{V_4}$,$\mathrm{V_5}$	III,$\mathrm{V_1}$,$\mathrm{V_2}$, $\mathrm{V_4}$,$\mathrm{V_5}$	III,$\mathrm{aV_L}$,$\mathrm{aV_F}$, $\mathrm{V_1}$,$\mathrm{V_2}$
6	I,II,III, $\mathrm{V_3}$,$\mathrm{V_4}$,$\mathrm{V_5}$	I,II,III, $\mathrm{V_3}$,$\mathrm{V_4}$,$\mathrm{V_5}$	I,III,$\mathrm{aV_L}$, $\mathrm{aV_F}$,$\mathrm{V_1}$,$\mathrm{V_2}$
7	II,$\mathrm{aV_R}$,$\mathrm{aV_L}$,$\mathrm{aV_F}$, $\mathrm{V_3}$,$\mathrm{V_4}$,$\mathrm{V_5}$	$\mathrm{aV_L}$,$\mathrm{aV_F}$,$\mathrm{V_1}$,$\mathrm{V_2}$, $\mathrm{V_3}$,$\mathrm{V_4}$,$\mathrm{V_5}$	III,$\mathrm{aV_R}$,$\mathrm{aV_L}$,$\mathrm{aV_F}$, $\mathrm{V_1}$,$\mathrm{V_3}$,$\mathrm{V_4}$
8	II,III,$\mathrm{aV_R}$,$\mathrm{aV_L}$, $\mathrm{V_3}$,$\mathrm{V_4}$,$\mathrm{V_5}$,$\mathrm{V_6}$	III,$\mathrm{aV_L}$,$\mathrm{aV_F}$,$\mathrm{V_1}$, $\mathrm{V_2}$,$\mathrm{V_3}$,$\mathrm{V_4}$,$\mathrm{V_5}$	I,III,$\mathrm{aV_L}$,$\mathrm{aV_F}$, $\mathrm{V_1}$,$\mathrm{V_3}$,$\mathrm{V_4}$,$\mathrm{V_5}$
9	I,II,III,$\mathrm{aV_R}$,$\mathrm{aV_F}$, $\mathrm{V_3}$,$\mathrm{V_4}$,$\mathrm{V_5}$,$\mathrm{V_6}$	II,III,$\mathrm{aV_L}$,$\mathrm{aV_F}$,$\mathrm{V_1}$, $\mathrm{V_2}$,$\mathrm{V_3}$,$\mathrm{V_4}$,$\mathrm{V_5}$	I,II,III,$\mathrm{aV_R}$,$\mathrm{aV_F}$, $\mathrm{V_1}$,$\mathrm{V_2}$,$\mathrm{V_3}$,$\mathrm{V_4}$
10	I,II,III,$\mathrm{aV_R}$,$\mathrm{aV_L}$, $\mathrm{aV_F}$,$\mathrm{V_2}$,$\mathrm{V_4}$,$\mathrm{V_5}$,$\mathrm{V_6}$	I,II,III,$\mathrm{aV_F}$,$\mathrm{V_1}$, $\mathrm{V_2}$,$\mathrm{V_3}$,$\mathrm{V_4}$,$\mathrm{V_5}$,$\mathrm{V_6}$	I,II,III,$\mathrm{aV_R}$,$\mathrm{aV_F}$, $\mathrm{V_1}$,$\mathrm{V_2}$,$\mathrm{V_3}$,$\mathrm{V_4}$,$\mathrm{V_5}$
11	I,II,III,$\mathrm{aV_R}$,$\mathrm{aV_F}$, $\mathrm{V_1}$,$\mathrm{V_2}$,$\mathrm{V_3}$,$\mathrm{V_4}$,$\mathrm{V_5}$,$\mathrm{V_6}$	I,II,III,$\mathrm{aV_R}$,$\mathrm{aV_L}$, $\mathrm{aV_F}$,$\mathrm{V_1}$,$\mathrm{V_2}$,$\mathrm{V_3}$,$\mathrm{V_4}$,$\mathrm{V_5}$	I,II,$\mathrm{aV_R}$,$\mathrm{aV_L}$,$\mathrm{aV_F}$, $\mathrm{V_1}$,$\mathrm{V_2}$,$\mathrm{V_3}$,$\mathrm{V_4}$,$\mathrm{V_5}$,$\mathrm{V_6}$
The most recurrent leads	II,$\mathrm{V_3}$	$\mathrm{V_1}$	III,$\mathrm{aV_F}$,$\mathrm{V_2}$

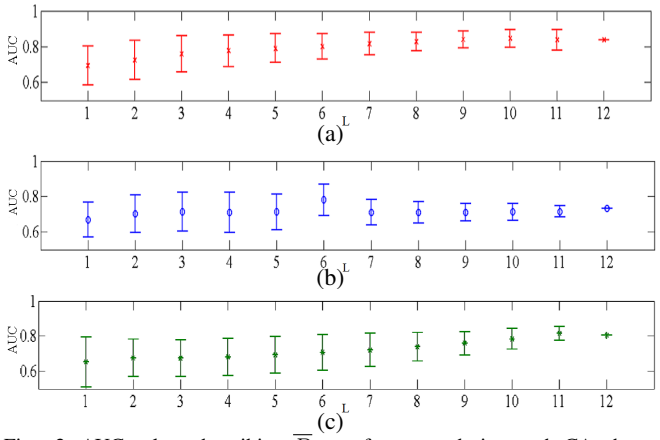

Fig. 2: AUC values describing $\overline{D}_L$ performance during each CA phase: (a) Before CA; (b) After PV isolation; (c) After CA.

concerned, it seems that the classifier best performs when 6 or 7 (and not 12) ECG leads are exploited. This phenomenon could be explained by the redefinition of electrical pathways subsequent to PV isolation and its transitory dynamics, in contrast with stable configurations typical of pre-operative and post-operative phases.

Table III shows that some leads recur in each subset: in most cases, the optimal L-lead subset is the same as that obtained at $(L-1)$, but with a further electrode introduced. As well as leads typically employed for AF analysis, e.g., V_1 and II, we can remark the presence of leads that are different from the precordial ones and describe heart electrical activity on the frontal plane. This evidence confirms the hypothesis that clinical information coming from multiple electrode locations can help ablation outcome prediction.

These results show that multilead ECG signals provide a broader overview of the atrial waveform pattern as compared to single leads, and that $\overline{D}_L$ can discriminate between successful and failing surgery actions in every moment of the procedure. Moreover, the multilead procedure described in Section II-D proves more robust to electrode selection than the single-lead approach of Section II-C. This feature may become particularly useful in scenarios where some leads do not provide an effective contribution to the recording, which could happen, e.g., if they get accidentally loose or disconnected from the patient's body.

A. Limitations of the Study

One of the main limits of this preliminary analysis is by the limited size of our persistent AF database. Secondly, validation of our results is affected by the lack of comparison with endocardial recordings. Actually, multilead ECG recordings provide a global outlook of heart activity, whereas endocardial signals account for local information. However, our attention was rather focused on surface signals, as we aimed at accomplishing our investigation with a non-invasive approach, so this context was not contemplated at all. The superiority of our atrial amplitude measure relative to more classical definitions such as the RMS value has been demonstrated in the context of non-invasive ablation-outcome prediction. Nevertheless, its performance in the presence of noise and interference not suppressed by the preprocessing filter remains to be investigated in more detail. Moreover, our analysis is not founded on a standard definition of CA clinical success. On the contrary, AF termination is assessed immediately after the treatment, neglecting possible recidive fibrillatory episodes beyond the temporal limit given in the "Methods" section. Finally, exclusive evaluation of the surgery could be hampered by several confusing factors, e.g., effects of cardioversion and/or drugs, post-operative oedemas, which can give their own contribution to the procedural outcome.

V. Conclusions

This work has put forward an automatic algorithm to compute f-wave amplitude that considerably reduces the subjectivity of manual analysis. In addition, a multilead extension based on PCA has been introduced and its superiority over single-lead perspective has been demonstrated. We have discriminated between successful and failing treatments before the therapy thanks to a new quantitative parameter depending on f-wave amplitude and taking into account all derivations. We have demonstrated that the spatio-temporal properties of the surface multilead ECG can quantitatively describe AF evolution and help in CA patient selection.

References

[1] A. Bollmann, D. Husser, L. Mainardi, F. Lombardi, P. Langley, A. Murray, J.J. Rieta, J. Millet, S.B. Olsson, M. Stridh, and L. Sörnmo. Analysis of surface electrocardiograms in atrial fibrillation: techniques, research, and clinical applications. *Europace*, 8(11):911–926, Nov. 2006.

[2] M. Haïssaguerre, P. Jaïs, D.C. Shah, A. Takahashi, M. Hocini, G. Quiniou, S. Garrigue, A. Le Mouroux, P. Le Metayer, and J. Clémenty. Spontaneous initiation of atrial fibrillation by ectopic beats originating in the pulmonary veins. *N. Engl. J. Med.*, 339:659–65, 1998.

[3] P. Jaïs, M. Haissaguerre, D.C. Shah, S. Chouairi, L. Gencel, M. Hocini, and J. Clémenty. A focal source of atrial fibrillation treated by discrete radiofrequency ablation. *Circulation*, 95:572–576, 1997.

[4] M. Haïssaguerre, P. Sanders, M. Hocini, P. Jaïs, and J. Clémenty. Pulmonary veins in the substrate for atrial fibrillation: the "venous wave" hypothesis. *J. Am. Coll. Cardiol.*, 43(12):2290–2292, Jun 2004.

[5] K. Nademanee, J. McKenzie, and E. Kosar et al. A new approach for catheter ablation of atrial fibrillation: mapping of the electrophysiologic substrate. *J. Am. Coll. Cardiol.*, 43(11):2044–53, 2004.

[6] H. Oral, A. Chug, Good E., A. Wimmer, S. Dey, N. Gadeela, et al. Radiofrequency catheter ablation of chronic atrial fibrillation guided by complex electrograms. *Circulation*, 115(20):2606–2612, 2007.

[7] I. Nault, N. Lellouche, S. Matsuo, S. Knecht, M. Wright, K.T. Lim, F. Sacher, P. Platonov, A. Deplagne, P. Bordachar, N. Derval, M.D. O'Neill, G.J. Klein, M. Hocini, P. Jaïs, J. Clémenty, and M. Haïssaguerre. Clinical value of fibrillatory wave amplitude on surface ECG in patients with persistent atrial fibrillation. *J. Interv. Card. Electrophysiol.*, 26(1):11–19, Oct. 2009.

[8] J. Pan and W. J. Tompkins. A real-time QRS detection algorithm. *IEEE Trans. Biomed. Eng.*, 3(3):230–236, 1985.

[9] A. Cabasson, O. Meste, G. Blain, and S. Bermon. A time delay estimation technique for overlapping signals in electrocardiograms. In *Proc. EUSIPCO*, Lausanne, Switzerland, Aug. 25-29 2008.

[10] F. Castells, P. Laguna, L. Sörnmo, A. Bollmann, and J. Millet Roig. Principal component analysis in ECG signal processing. *EURASIP Journal on Advances in Signal Processing*, 2007:21 pages, 2007.

[11] P. Bonizzi, O. Meste, V. Zarzoso, D. G. Latcu, I. Popescu, P. Ricard, and N. Saoudi. Atrial fibrillation disorganization is reduced by catheter ablation: A standard ECG study. In *Proc. IEEE EMBS 2010*, pages 5286–5289, 2010.

[12] P. Bonizzi, M. S. Guillem, A. M. Climent, J. Millet, V. Zarzoso, F. Castells, and O. Meste. Noninvasive assessment of the complexity and stationarity of the atrial wavefront patterns during atrial fibrillation. *IEEE Trans. Biomed. Eng.*, 57(9):2147–2157, 2010.